Introduction

Pancreatic adenocarcinoma is the fourth leading cause of cancer death worldwide [1]. Despite recent advances in diagnostic techniques, pancreatic adenocarcinoma is diagnosed at an advanced stage in most patients and, consequently, the overall 5-year survival rate is <5 % [2]. Thus, the development of a new treatment option is needed to improve the prognosis of pancreatic cancer patients without toxicity.

Immunotherapy is one of the most attractive therapies as a new treatment procedure for melanoma and other solid tumors [3]. Recent technical advances have enabled the identification of various tumor-associated antigens (TAAs) [4–21]; however, few of their epitopes are inducers of cytotoxic T lymphocyte (CTL) responses against tumors [22]. Several kinds of epitope have also been identified in patients with pancreatic adenocarcinoma [23, 24]. However, previous studies focused on the identification and evaluation of a particular antigen, and different TAAs have not yet been compared simultaneously; therefore, little is known about which epitope is the most immunogenic and useful in eliciting clinical responses in pancreatic adenocarcinoma patients.

In the present study, we compared CTL responses with various TAA-derived epitopes in identical patients with pancreatic adenocarcinomas and examined the factors that affect immune responses. This approach provided information that is useful for selecting immunogenic TAAs and suitable patients and developing a new immunotherapy for pancreatic adenocarcinoma.

Materials and methods

Patients and clinical information

In this study, we examined 41 HLA-A24-positive patients with pancreatic adenocarcinoma and 14 healthy volunteers who were HLA-A24-positive, but did not have any cancers, as negative controls. Fine-needle biopsy, a surgical specimen, or autopsy was used for the pathological diagnosis of pancreatic adenocarcinoma in 18 patients. Diagnosis of the remaining 23 patients was achieved using the radiological findings of computed tomography and/or magnetic resonance imaging. We investigated patient background, treatment procedures, and outcomes.

Clinical information was obtained from the medical records of patients. We evaluated the tumor stage using TNM staging of the Union Internationale Contre Le Cancer (UICC) system (7th version) (UICC stage). The frequency of lymphocyte subsets was calculated by dividing the absolute lymphocyte count by the absolute leukocyte count. HLA typing of peripheral blood mononuclear cells (PBMCs) from patients and healthy volunteers was performed by the reverse sequence-specific oligonucleotide with polymerase chain reaction (PCR-RSSO). This study was approved by the Ethics Committees of Kanazawa University (No. 1237) and Kanazawa Medical Center (No. 17), and all patients gave written informed consent to participate in accordance with the Helsinki Declaration.

Table 1 Peptides used in this study

Peptide No.	TAA	Amino acid sequence	Reference
1	$ART1_{188}$	EYCLKFTKL	[14]
2	$ART4_{161}$	AFLRHAAL	[11]
3	$ART4_{899}$	DYPSLSATDI	[11]
4	$Cyp\text{-}B_{109}$	KFHRVIKDF	[7]
5	$Cyp\text{-}B_{315}$	DFMIQGGDF	[7]
6	Lck_{208}	HYTNASDGL	[8]
7	Lck_{488}	DYLRSVLEDF	[8]
8	$MAGE\text{-}A1_{135}$	NYKHCFPEI	[6]
9	$MAGE\text{-}A3_{195}$	IMPKAGLLI	[16]
10	$SART1_{690}$	EYRGFTQDF	[12]
11	$SART2_{899}$	SYTRLFLIL	[13]
12	$SART3_{109}$	VYDYNCHVDL	[21]
13	$Her\text{-}2/neu_{8}$	RWGLLLALL	[17]
14	$p53_{161}$	AIYKQSQHM	[18]
15	$p53_{204}$	EYLDDRNTF	[5]
16	$MRP3_{765}$	VYSDADIFL	[20]
17	$MRP3_{503}$	LYAWEPSFL	[20]
18	$hTERT_{461}$	VYGFVRACL	[4]
19	$hTERT_{324}$	VYAETKHFL	[4]
20	$WT\text{-}1_{235}$	CMTWNQMNL	[15]
21	$VEGFR2_{169}$	RFVPDGNRI	[19]
22	$VEGFR1_{1084}$	SYGVLLWEI	[10]
23	$survivin2B_{80}$	AYACNTSTL	[9]
24	HIV env_{584}	RYLRDQQLL	[25]
25	CMV $pp65_{328}$	QYDPVAALF	[26]

Synthetic peptides and preparation of PBMCs

The 23 epitopes derived from 17 different TAAs used in the present study are listed in Table 1. We selected epitopes that had previously been identified as HLA-A24-restricted and suggested to have immunogenicity in various cancers not restricted to pancreatic cancer [4–21]. Epitopes derived from the HIV envelope protein (HIV env_{584}) [25] and cytomegalovirus (CMV) pp65 (CMV$pp65_{328}$) [26] were also used to assess T cell responses. Peptides were synthesized at Mimotope (Melbourne, Australia), Sumitomo Pharmaceuticals (Osaka, Japan), COSMO BIO Co. (Tokyo, Japan), and Scrum Inc. (Tokyo, Japan). Purities were determined to be >80 % by analytical high-performance

liquid chromatography (HPLC). PBMCs were separated as described below; heparinized venous blood was diluted in phosphate-buffered saline (PBS) and loaded on Ficoll-Histopaque (Sigma, St. Louis, MO) in 50-ml tubes. After centrifugation at 2,000 rpm for 20 min at room temperature, PBMCs were harvested from the interphase, resuspended in PBS, centrifuged at 1,400 rpm for 10 min, and finally resuspended in complete culture medium consisting of RPMI (GibcoBRL, Grand Island, NY), 10 % heat-inactivated FCS (Gibco BRL), 100 U/ml penicillin, and 100 μg/ml streptomycin (Gibco BRL).

Cell lines

The HLA-A*2402 gene-transfected C1R cell line (C1R-A24) was cultured in RPMI 1640 medium containing 10 % FCS and 500 μg/ml hygromycin B (Sigma, St. Louis, MO), and K562 was cultured in RPMI 1640 medium containing 10 % FCS [27]. MiaPaca2, AsPC1, BxPC3, Panc-1, CAPAN1, and CAPAN2 were purchased from the American Type Culture Collection (VA, USA). YPK-1 and YPK-2 were kind gifts from Prof. Oka and Dr. Yoshimura (Yamaguchi University Graduate School of Medicine, Yamaguchi, Japan). PK-1 was provided by the RIKEN BRC through the National Bio-Resource Project of MEXT, Japan. Human pancreatic cancer cell lines were cultured in DMEM (GibcoBRL) or RPMI 1640 medium containing 10 % fetal calf serum (FCS). All media contained 100 U/mL penicillin and 100 μg/mL streptomycin.

RNA preparation and real-time PCR

The expression of TAA messenger RNA (mRNA) in human pancreatic cancer cell lines and pancreatic adenocarcinoma tissues was analyzed by real-time polymerase chain reaction (PCR). Cell lines were harvested, centrifuged, and washed with PBS, and total RNA was then isolated using Quick-Gene (Fuji Film, Tokyo). Total RNA from frozen pancreatic adenocarcinoma samples was isolated using a GenElute Mammalian Total RNA Miniprep Kit (Sigma-Aldrich) according to the manufacturer's protocol. cDNA was synthesized from 150 ng of total RNA using a high-capacity cDNA reverse transcription kit (PE Applied Biosystems, CA, USA) and was then mixed with TaqMan Universal Master Mix (PE Applied Biosystems) and each TaqMan probe. Primer pairs and probes for various TAAs and β-actin were obtained from the TaqMan assay reagents library. Thermal cycling conditions were 25 °C for 10 min, 37 °C for 120 min, and 85 °C for 1 min. cDNA was subjected to quantitative real-time PCR analyses targeting various TAAs and β-actin. Analyses were performed using the StepOne Real-Time PCR system and StepOne v2.0 software. Relative gene expression values were determined. Data are presented as fold differences in TAA expression normalized to the housekeeping gene β-actin as an endogenous reference.

Enzyme-linked immunospot assay (ELISPOT assay)

Ninety-six-well plates (Millititer, Millipore, Bedford, MA) were coated with anti-human interferon-γ (IFN-γ) (Mabtech, Nacka, Sweden) at 4 °C overnight and then washed 4 times with sterile PBS. The plates were then blocked with RPMI 1640 medium containing 5 % FCS for 2 h at room temperature. A total of 300,000 unfractionated PBMCs were added in duplicate cultures of RPMI 1640 containing 5 % FCS together with the peptides at 10 μg/ml. After 24 h, the plates were washed 8 times with PBS and incubated overnight with 100 μl of the biotin-conjugated anti-human IFN-γ antibody. After another 4 washes with PBS, streptavidin-AP was added for 2 h. Finally, the plates were washed again 4 times with PBS and developed with freshly prepared NBT/BCIP solution (Biorad, Hercules, CA). The reaction was stopped by washing with distilled water and drying at room temperature. Colored spots with fuzzy borders, which indicated the presence of IFN-γ-secreting cells, were counted. The number of specific spots was determined by subtracting the number of spots in the absence of the antigen. Responses were considered positive if 10 or more specific spots were detected and if the number of spots in the presence of an antigen was at least two-fold than that in its absence.

Peptide-specific CTL induction and cytotoxicity assay

Synthetic peptide-specific T cells were expanded from PBMCs in 96-well round-bottom plates (NUNC, Naperville, IL). Four hundred thousand cells/well were stimulated with synthetic peptides at 10 μg/ml, 10 ng/ml rIL-7, and 100 pg/ml rIL-12 (Sigma) in RPMI 1640 supplemented with 10 % heat-inactivated human AB serum, 100 U/ml penicillin, and 100 μg/ml streptomycin. The cultures were restimulated with 10 μg/ml peptide, 20 U/ml rIL-2 (Sigma), and 10^5 mitomycin C-treated autologous PBMCs as feeder cells on days 7 and 14. One hundred microliters of RPMI medium with 10 % human Ab serum and rIL-2 at a final concentration of 10 U/ml were added to each well on days 4, 11, and 18. The cytotoxicity assay was conducted on day 22.

The C1R-A24 and human pancreatic cancer cell lines were used as target cells for the ^{51}Cr release assay. C1R-A24 cells were incubated overnight with 10 μg/ml synthetic peptides and labeled with 25 μCi of ^{51}Cr for 1 h. Pancreatic cancer cell lines were also labeled with 25 μCi of ^{51}Cr for 1 h without incubation with peptides. After three washes with PBS, target cells were plated at 3,000 cells/well in complete medium

in round-bottom 96-well plates. Unlabeled K562 (120,000 cells/well) was added to reduce non-specific lysis. Peptide-stimulated PBMCs were added at various effector-to-target ratios as indicated. Maximum release was determined by the lysis of ^{51}Cr-labeled targets with 5 % Triton X-100 (Sigma Chemical). Spontaneous release was <10 % of maximum release for all experiments, except for when it was <15 % when the target cells were human pancreatic cancer cell lines. Percent-specific cytotoxicity was determined using the following formula: 100 × (experimental release − spontaneous release)/(maximum release − spontaneous release), and specific cytotoxic activity was calculated as follows: (cytotoxic activity in the presence of the peptide) − (cytotoxic activity in the absence of the peptide). Specific cytotoxicity of more than 10 % was considered to be positive.

Tetramer staining and flow cytometry

TAA-specific tetramers were purchased from Medical Biological Laboratories Co., Ltd. (Nagoya, Japan). Tetramer staining was performed as described below. One million isolated PBMCs or peptide-specific CTLs pulsed with TAA-derived peptides were washed, resuspended in 200 μl of PBS without calcium or phosphate, and stained with 40 μg/ml tetrameric complexes and monoclonal antibodies against cell surface proteins for 30 min at room temperature. The following monoclonal antibodies were used: anti-CD8-APC (BD PharMingen, San Diego, CA), anti-CCR7-FITC, anti-CD45RA-PerCP, and tetramer-PE. Cells were washed, fixed with 0.5 % paraformaldehyde/PBS, and analyzed on a Becton–Dickinson FACSAria II system.

Statistical analysis

Fisher's exact test and unpaired Student's *t* test were used to analyze the effect of variables on immune responses in pancreatic cancer patients. Overall survival was calculated from the day of pancreatic cancer diagnosis until the date of death or the last day of the follow-up period. Cumulative survival proportions were calculated using the Kaplan–Meier method, and any differences were evaluated using the log-rank test. A p value of <0.05 was considered to be significant, and all the tests were two-sided. All statistical analyses were performed using the SPSS statistical software program package (SPSS version 11.0 for Windows).

Results

Patients

Patient characteristics are summarized in the Supplementary Table. The median age of patients was 72 years, and patients included 24 males (59 %). The main localization of the tumors was the pancreatic head in 39 % of patients and the pancreatic body or tail in 61 %. The majority of patients (93 %) had advanced-stage cancer, namely, UICC stage III or IV. Therapeutic procedures mainly involved chemotherapy consisting of protocols such as gemcitabine monotherapy, S-1 monotherapy, or a combination of both drugs. Only 11 patients received the best supportive therapy to relieve physical and spiritual pain. A total of 61 % of patients had died by the last day of the follow-up period, and the median overall survival time of patients was 7.2 months.

TAA expression in pancreatic cancer cell lines and human cancer tissues

We evaluated the expression of 17 different TAAs in 9 human pancreatic cancer cell lines using real-time PCR. Although differences were observed from cell to cell, TAAs were expressed in more than 40 % of pancreatic adenocarcinoma cell lines, except for adenocarcinoma antigens recognized by T cells (ART)1 (11 %) and ART4 (33 %) (Table 2). We then investigated TAA expression in 7 surgical and 5 autopsy specimens. The expression of most TAAs in pancreatic adenocarcinoma specimens was similar to or more frequent than that in human pancreatic cancer cell lines, except for melanoma-associated antigen (MAGE)-A1 and MAGE-A3 (Table 2).

Detection of TAA-specific T cells by IFN-γ ELISPOT analysis

IFN-γ ELISPOT responses were evaluated with PBMCs to determine how frequently T cells respond to TAA-derived peptides and control peptides in patients with pancreatic adenocarcinoma (Fig. 1a). Positive responses to at least one TAA-derived peptide were observed in 28 of 41 (68 %) patients. On the other hand, 14 of 23 (61 %) peptides were recognized by T cells obtained from at least one patient. $ART1_{188}$, $ART4_{161}$, $ART4_{899}$, lymphocyte-specific protein tyrosine kinase $(Lck)_{208}$, $MAGE\text{-}A3_{195}$, $p53_{161}$, human telomerase reverse transcriptase $(hTERT)_{461}$, $hTERT_{324}$, Wilms tumor $(WT)\text{-}1_{235}$, vascular endothelial growth factor receptor $(VEGFR)2_{169}$, and $VEGFR1_{1084}$ were recognized in more than two patients, which suggested that these peptides have the potential to be immunogenic. Peptides 24 ($HIVenv_{584}$) and 25 ($CMVpp65_{328}$) were recognized in 0 and 38 % of patients, respectively.

Peptides $ART4_{161}$, $ART4_{899}$, Cyclophilin B $(Cyp\text{-}B)_{315}$, Lck_{208}, $hTERT_{324}$, and $VEGFR1_{1084}$ were recognized in more than one healthy volunteer, and/or the percentage of positive responses was higher in healthy volunteers than in pancreatic adenocarcinoma patients, which indicated

Table 2 Expression of various TAAs mRNA in pancreatic cancer cell lines and pancreatic cancer tissues measured by real-time PCR

TAA	Primer	Positive cell lines/ cell lines tested *n* (%)	Positive specimens/ specimens tested *n* (%)
ART1	Hs00188841_m1	1/9 (11)	5/12 (42)
ART4	Hs00221465_m1	3/9 (33)	11/12 (92)
CypB	Hs00168719_m1	9/9 (100)	12/12 (100)
Lck	Hs00178427_m1	8/9 (89)	11/12 (92)
MAGEA1	Hs00607097_m1	4/9 (43)	1/12 (8)
MAGEA3	Hs00366532_m1	4/9 (43)	1/12 (8)
SART1	Hs00193002_m1	9/9 (100)	12/12 (100)
SART2	Hs00203441_m1	9/9 (100)	12/12 (100)
SART3	Hs00206829_m1	9/9 (100)	12/12 (100)
HER2/neu	Hs00170433_m1	9/9 (100)	12/12 (100)
p53	Hs00153340_m1	9/9 (100)	12/12 (100)
MRP3	Hs00358656_m1	9/9 (100)	12/12 (100)
hTERT	Hs00162669_m1	9/9 (100)	9/12 (75)
WT-1	Hs00240913_m1	5/9 (56)	9/12 (75)
VEGFR2	Hs00911700_m1	5/9 (56)	11/12 (92)
VEGFR1	Hs01052961_m1	6/9 (67)	12/12 (100)
Survivin	Hs00153353_m1	9/9 (100)	12/12 (100)

that the responses to these peptides were not specific to T cells from patients with pancreatic adenocarcinoma (Fig. 1b). In other words, peptides $ART1_{188}$, MAGE-$A3_{195}$, $p53_{161}$, $hTERT_{461}$, WT-1_{235}, and $VEGFR2_{169}$ have specific immunogenic potential in patients with pancreatic adenocarcinoma.

The number of peptide-specific IFN-γ-producing T cells was counted to examine the frequency of T cells responsive to TAA-derived peptides. A range of 10–46 T cells per 300,000 PBMCs in patients with pancreatic adenocarcinoma produced IFN-γ (Fig. 1c).

TAA-specific CTL induction and cytotoxic activity

We attempted to induce peptides specific to CTLs from the PBMCs of pancreatic adenocarcinoma patients. Cytotoxicity assays were performed in more than five patients for each peptide. Of the 11 peptides recognized in more than two patients in the IFN-γ ELISPOT assay, 6 peptides (MAGE-$A3_{195}$, $p53_{161}$, $hTERT_{461}$, $hTERT_{324}$, WT-1_{235}, and $VEGFR2_{169}$) could induce their specific CTLs, which were confirmed to be able to respond to C1RA24 cells pulsed with corresponding peptides by the cytotoxicity assay, as shown in Fig. 2a.

We conducted a cytotoxicity assay to determine whether peptide-specific CTLs from healthy volunteers could show their cytotoxic activity against pancreatic carcinoma cell lines. $P53_{161}$-, $hTERT_{461}$-, and $hTERT_{324}$-specific CTLs showed cytotoxicity against YPK-2 (HLA-A24-, p53-, and hTERT-positive), but not against Panc-1 (HLA-A24-negative, p53- and hTERT-positive). MAGE-$A3_{195}$-, WT-1_{235}-, and $VEGFR2_{169}$-specific CTLs also showed cytotoxic activity against YPK-2 (HLA-A24-, MAGE-A3-, WT-1-, and VEGFR2-positive), but not against YPK-1 (HLA-A24-positive, MAGE-A3-, WT-1-, and VEGFR2-negative). Representative data are shown in Fig. 2b.

Phenotypic analysis of TAA-derived peptides specific to T cells

To analyze the characteristics of TAA-derived peptides specific to T cells and select the appropriate epitope for immunotherapy in patients with pancreatic adenocarcinoma, we performed phenotypic analysis by tetramer staining and FACS analysis. We first attempted to detect MAGE-$A3_{195}$-, $hTERT_{461}$-, and WT-1_{235}-specific tetramer-positive T cells in PBMCs and CTLs induced by the corresponding peptides in healthy volunteers. The ratio of tetramer-positive T cells was increased in CTLs and their frequencies were 1.481–2.930 % of $CD8^+$ T cells, suggesting that these tetramers work well (Fig. 3a). We also conducted similar assays in pancreatic adenocarcinoma patients and detected tetramer-positive T cells in CTLs (Fig. 3b).

We then examined the naïve/effector/memory phenotype of tetramer-positive cells in the PBMCs of patients. The memory phenotype was investigated by the criterion of CD45RA/CCR7 expression [28]. In tetramer analysis, the frequencies of MAGE-$A3_{195}$-, $hTERT_{461}$-, and WT-1_{235}-specific tetramer-positive T cells were 0.003–0.044,

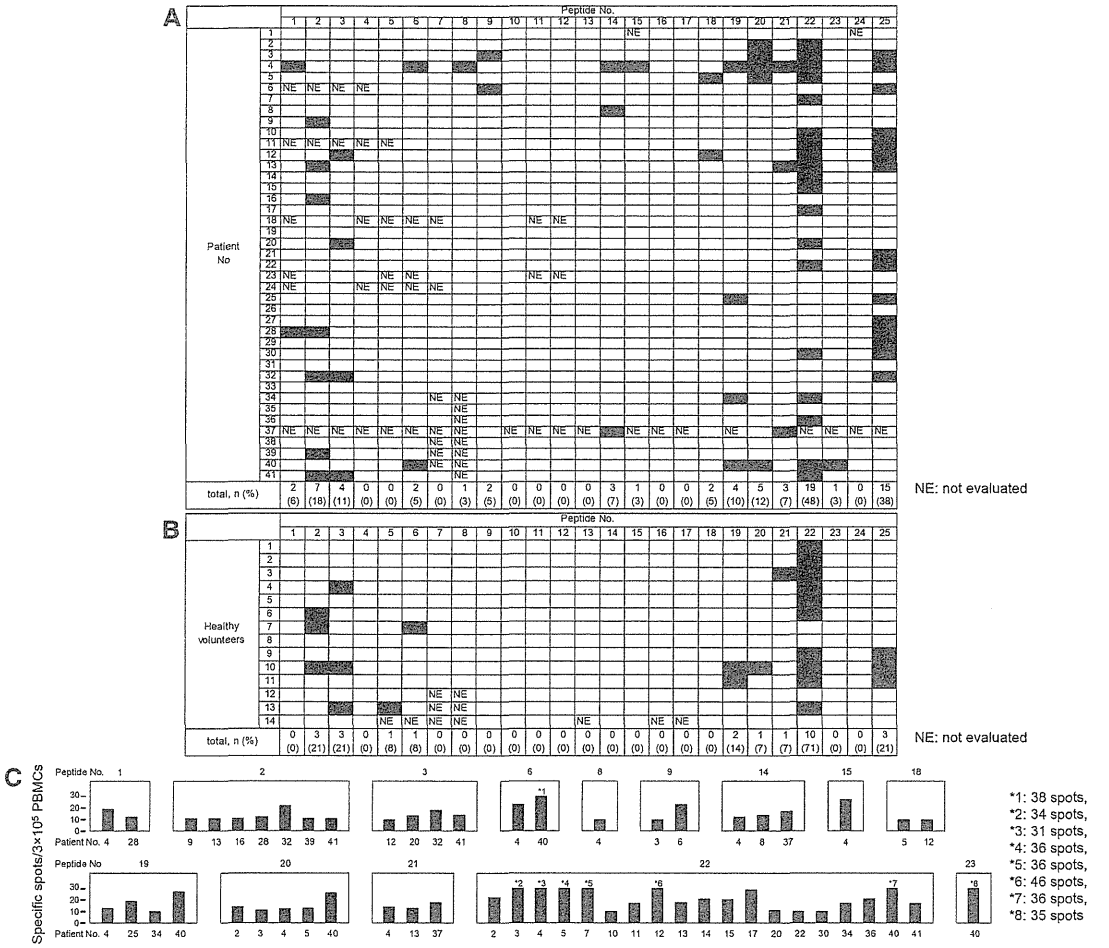

Fig. 1 T cell responses to TAA-derived peptides and control peptides in pancreatic adenocarcinoma patients **a** and healthy volunteers **b**. T cell responses were evaluated by the IFN-γ ELISPOT assay. Responses were considered positive if 10 or more specific spots were detected and if the number of spots in the presence of an antigen was at least twofold that in its absence. *Black boxes* indicate positive responses. **c** The frequency of TAA-specific IFN-γ-producing T cells evaluated by the ELISPOT assay. *Black bars* indicate the response of one patient

0.006–0.053, and 0.030–0.191 % of $CD8^+$ T cells, respectively. The frequency of $CD45RA^-/CCR7^+$ (central memory), $CD45RA^-/CCR7^-$ (effector memory), and $CD45RA^+/CCR7^-$ (effector) T cells in tetramer-positive cells depended on the patient and all phenotypes were observed in all patients, except for patients 1, 8, 28, 29, and 4 (Supplementary Fig. 1).

TAA-specific T cell responses and clinical features of pancreatic cancer patients

In the present study, we analyzed the clinical features that can affect TAA-specific immune responses. When we divided patients into two groups based on their frequencies of lymphocyte subsets in peripheral leukocytes (<24 %, the median value among all patients, or equal to or more than 24 %) and the strength of TAA-specific immune responses into three groups according to the frequency of TAA-specific T cells (<10 specific spots on ELISPOT assays, no response; 10–19 specific spots, weak response; equal to or more than 20 specific spots, strong response), the patients with more lymphocyte subsets in peripheral leukocytes showed stronger TAA-specific T cell responses (Supplementary Fig. 2). On the other hand, we could not find any relationship between TAA-specific immune responses and other clinical characteristics such as age, sex, tumor marker levels, UICC stage, or metastasis status.

We also analyzed the correlation between T cell responses and the prognosis of pancreatic cancer patients. The median overall survival time of patients with T cell responses to at least one TAA-derived peptide evaluated

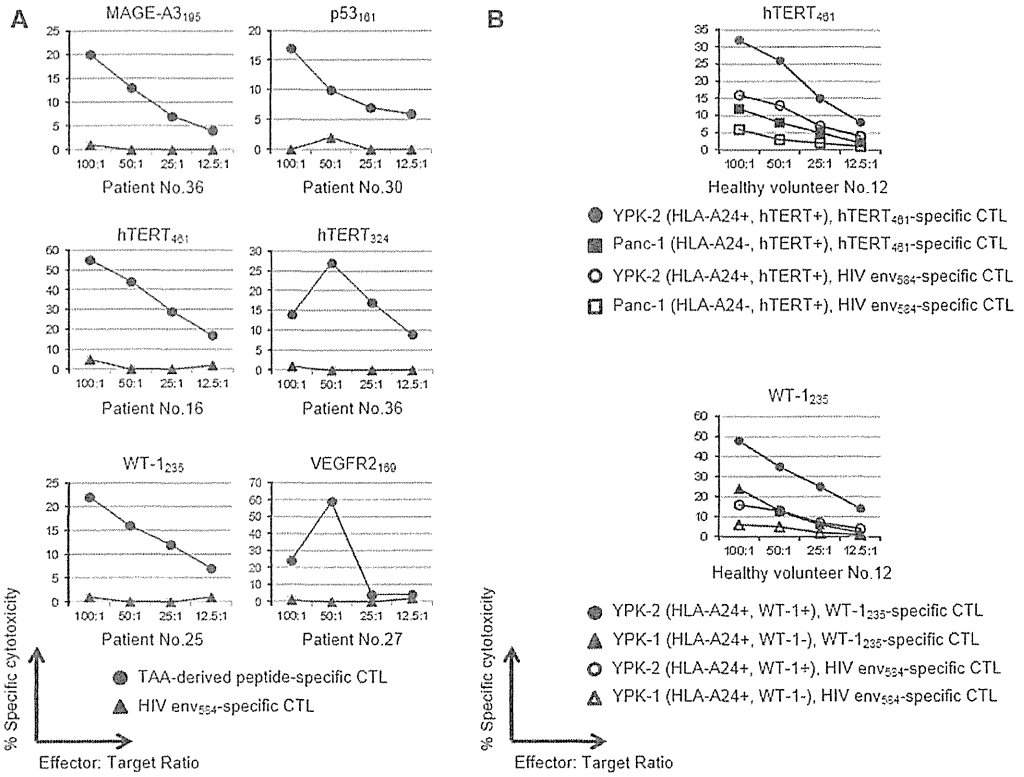

Fig. 2 **a** T cell responses to peptides evaluated by the cytotoxicity assay. Peptide-specific CTL induction and cytotoxicity assays were performed on the PBMCs from at least five patients, and representative data are shown when peptide-specific CTLs were induced in one or more patients. A percent-specific cytotoxicity of more than 10 % was considered to be positive. Six peptides: 9, 14, 18, 19, 20, and 21, could induce their specific CTLs, and these could respond to CIRA24 cells pulsed with the corresponding peptides in the cytotoxicity assay. **b** Cytotoxic activity against the pancreatic carcinoma cell lines of TAA-specific CTLs from healthy volunteers evaluated by the cytotoxicity assay. Cytotoxicity was stronger against pancreatic carcinoma cells that were HLA-A24-restricted and expressed corresponding TAAs than against those not HLA-A24-restricted or not expressing corresponding TAAs

by the ELISPOT assay was 12.2 months, which was significantly longer than that without T cell responses (4.3 months) ($p = 0.013$) (Fig. 4a). On the other hand, no correlation was observed between positive T cell responses and CMV-derived peptides and clinical outcomes (Fig. 4b), suggesting that TAA-specific T cell responses, but not the general immune response, is a prognostic factor in patients with pancreatic adenocarcinoma. The frequencies of regulatory T cells or the ratio of regulatory T cells to $CD8^+$ T cells had no impact on the outcomes of patients in this study.

Discussion

Immunotherapy is considered to be a fourth treatment procedure for cancer following surgical resection, radiotherapy, and chemotherapy [29]. Cancer vaccine therapy was previously shown to convey survival benefits to prostate cancer patients in a clinical phase III trial [30], and some candidates of other cancers have been identified and separately evaluated to determine whether a CTL response can be elicited, with the subsequent elimination of cancer cells and improvement in outcomes. Although a successful clinical response depends on how much tumor antigens elicit their specific CTLs, which are the most important effector cells for antitumor immune responses, to the best of our knowledge, no studies have attempted to identify which epitopes are optimal for peptide vaccine therapy in patients with pancreatic adenocarcinoma. Therefore, we simultaneously compared peptide-specific T cell responses among various TAAs in 41 identical patients with pancreatic adenocarcinoma under the same experimental conditions.

Therapeutic function is the most important factor to consider when determining the usefulness of cancer antigens for peptide vaccine therapy. However, it is very difficult to compare the efficacy of more than one epitope, especially in patients with pancreatic adenocarcinoma whose survival time is very short. Under such circumstances, immunogenicity, specificity, oncogenicity, expression levels, % of

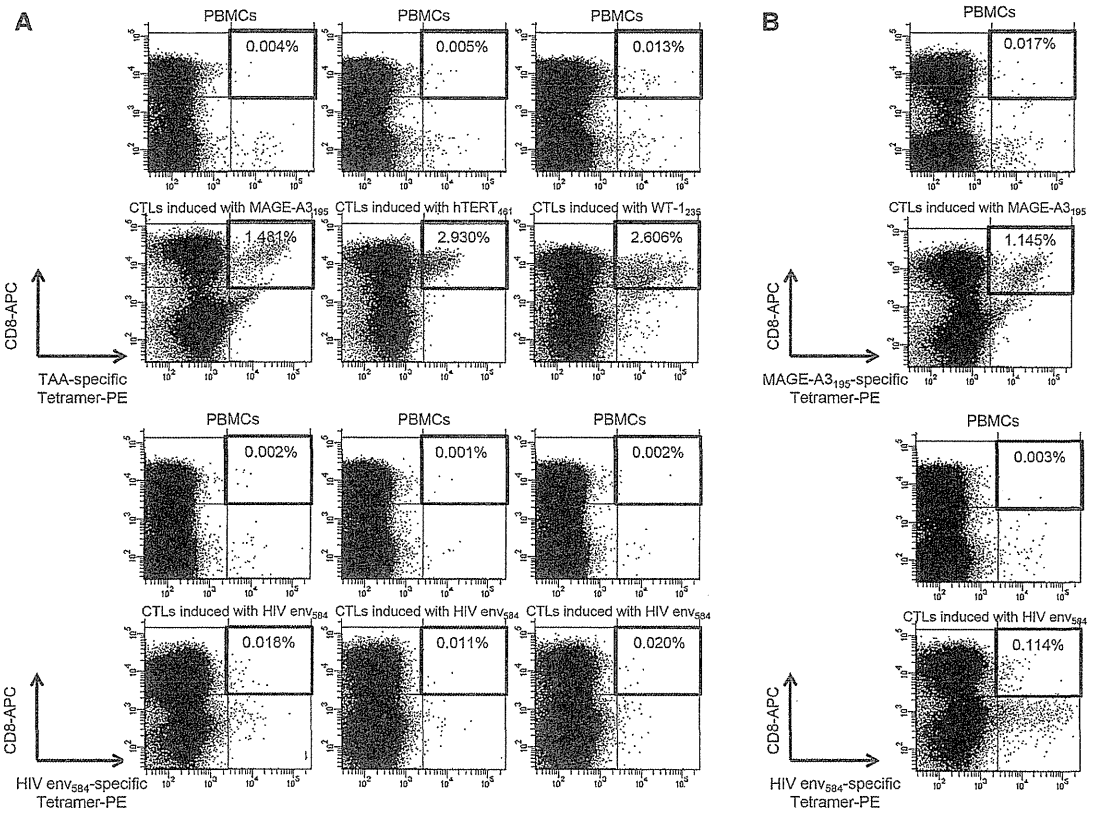

Fig. 3 Detection of TAA-specific, HLA-A24-tetramer$^+$, and CD8$^+$ lymphocytes in PBMCs from healthy volunteers and pancreatic adenocarcinoma patients. **a** Tetramer analyses were performed on eight healthy volunteers for each peptide (MAGE-A3$_{195}$, hTERT$_{461}$, and WT-1$_{235}$). Tetramer$^+$ and CD8$^+$ T cells were detectable in both PBMCs and CTLs induced by their corresponding peptides in at least one healthy volunteer, and representative data are shown in cases in which the ratio of tetramer$^+$ and CD8$^+$ T cells to CD8$^+$ T cells was higher in CTLs induced with each TAA-derived peptide than in PBMCs. **b** Tetramer analyses were performed on pancreatic adenocarcinoma patients using PBMCs and CTLs, which were induced with TAA-derived peptides and showed cytotoxicity against pancreatic cancer cell lines in cytotoxicity assay. Levels of tetramer$^+$ and CD8$^+$ T cells were higher in CTLs induced with TAA-derived peptides than in PBMCs. Representative data are shown in cases in which the ratio of tetramer$^+$ and CD8$^+$ T cells to CD8$^+$ was 0.017 % in PBMCs and 1.145 % in MAGE-A3$_{195}$-specific CTLs

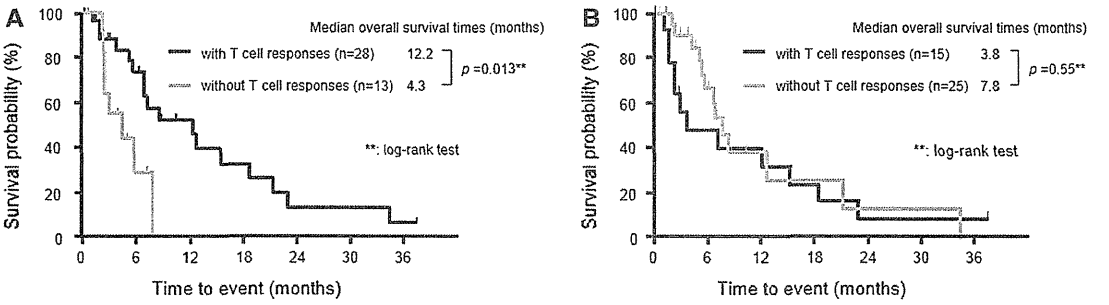

Fig. 4 Kaplan-Meier plot of the overall survival of pancreatic cancer patients according to **a** TAA-specific T cell responses and **b** T cell responses to CMV-derived peptides. **a** TAA-specific T cell responses were defined as positive if 10 or more specific spots to at least one TAA-derived peptide were detected on the ELISPOT assay. The overall survival time of patients with TAA-specific T cell responses was significantly longer than that of patients without TAA-specific T cell responses. **b** T cell responses to CMV-derived peptides were defined as positive if 10 or more specific spots to CMV-derived peptides were detected on ELISPOT assays. No correlation was observed between positive T cell responses to CMV-derived peptides and the clinical outcomes of patients

positive cells, and the number of patients with antigen-positive cancer are considered to be alternative criteria [31]. On the basis of our results, $p53_{161}$, $hTERT_{461}$, $WT\text{-}1_{235}$, and $VEGFR2_{169}$ are considered the most optimal epitopes that satisfy all of the above criteria for peptide vaccine therapy in pancreatic adenocarcinoma patients. Although MAGE-$A3_{195}$ showed immunogenicity, its expression did not appear to be high in pancreatic adenocarcinoma tissue [32]. Therefore, it may be a candidate for cancer vaccine therapy when MAGE-A3 is confirmed to be overexpressed in pancreatic cancer tissue.

A mutation in the p53 gene and overexpression of the p53 protein have been reported previously in pancreatic adenocarcinoma [33], and all pancreatic cancer cell lines and specimens used in our study expressed p53. Some strategies targeting p53 have been proposed over the last decade [34]. As peptide vaccine therapy, the wild-type p53 peptide is well preserved in mutant p53 because most mutations in the p53 gene are missense mutations, and are considered to be one of the attractive targets as a cancer antigen. The frequencies of the CTL response against HLA-A24-restricted $p53_{161}$ investigated by the ELISPOT assay in head and neck carcinoma and hepatocellular carcinoma were shown to be 35 and 10 %, respectively [35, 36]. Although the frequency of 7 % in our study is lower, given the difference according to the primary tumor site or balance between sensitivity and specificity, induced CTLs showed cytotoxic activity against pancreatic adenocarcinoma cell lines, which suggested that p53 may be an attractive target in patients with pancreatic cancer.

hTERT is widely overexpressed in various cancer cells including pancreatic cancer [37], which is consistent with our results. A clinical trial demonstrated that GV1001, a HLA class II epitope corresponding to the hTERT (611–626) fragment, was immunogenic in pancreatic cancer patients [38]. Another previous study evaluating T cell responses to several hTERT epitopes in patients with hepatocellular carcinoma [39] demonstrated that $hTERT_{461}$- and $hTERT_{324}$-specific CTLs were induced in 5 (6.9 %) and 9 (12.5 %) of 72 patients, respectively. In the current study, these frequencies were equivalent and the killing of pancreatic cancer cell lines was demonstrated, which suggested that these epitopes also had immunogenicity in pancreatic cancer patients.

Peptide vaccine therapies using $WT\text{-}1_{235}$ and $VEGFR2_{169}$ combined with gemcitabine have already been conducted in pancreatic adenocarcinoma patients [23, 24]. We clarified that $WT\text{-}1_{235}$- and $VEGFR2_{169}$-specific CTLs induced from PBMCs showed cytotoxicity for human pancreatic cancer cell lines, and the results of further investigations are anticipated.

We performed phenotypic analysis of TAA-derived epitope-specific T cells to determine the most appropriate epitope for immunotherapy in patients with pancreatic adenocarcinoma. Epitope-specific tetramer$^+$ cells in PBMCs were also found in patients without IFN-γ ELISPOT responses, which was consistent with the findings of previous studies [39, 40] and suggested the existence of dysfunctional epitope-specific T cells. Epitope-specific tetramer$^+$ cells were also identified at a very low frequency in PBMCs from healthy volunteers and increased in CTLs induced with TAA-derived peptides, which was also consistent with previous studies in which TAA-specific tetramer$^+$ T cells were detectable in samples from healthy donors [41] or the in vitro stimulation of PBMCs with the epitopes derived from TAA could induce TAA-specific CTLs in healthy volunteers [42], even though the precise mechanism has not yet been clarified. Phenotypic analysis showed that the frequency of T cells with each memory and effector phenotype depended on the patient and also that peptide-specific memory T cells existed in PBMCs of patients with pancreatic adenocarcinoma. Because T cells with the memory phenotype exert stronger antitumor effects by secondary stimulation with the antigen, our results suggest that an additional immunological approach such as that consisting of a TAA-derived protein or peptide, recombinant virus, and engineered tumor cells to boost T cell function may be useful to enhance host antitumor immune responses.

Another purpose of this study was to identify the factors influencing immune responses. Our results suggested that the frequencies of the lymphocyte subsets in peripheral leukocytes were very important in the induction of TAA-specific CTLs. Although the relationship between cancer, inflammation, and immunity has already been documented [43], the precise mechanism has yet to be fully understood. One of the speculated reasons why PBMC from patients with lymphocytopenia could not induce a good immune response in our study is that the release of inhibitory immunological cytokines such as transforming growth factor β or IL-10 from pancreatic adenocarcinoma tissue decreases lymphocyte counts and impairs the function of lymphocytes both systemically and in the microenvironment [44]. It was also reported that lymphocyte counts and CTL responses were prognostic markers in advanced cancer cases receiving peptide vaccine therapy [45, 46]. Our results showing a correlation between the T cell response and outcomes in pancreatic adenocarcinoma patients corresponded to these previous findings, which indicate that restricting the objective to those with an adequate lymphocyte subset could lead to a clinical trial with favorable outcomes.

A limitation of this study was the lack of data for the clinical response. Tumor shrinkage or survival benefits are not always observed in all patients who exhibit immune responses. Further, clinical studies using peptides that could induce TAA-specific CTLs are needed to confirm our findings.

In conclusion, we simultaneously compared T cell responses to various TAA-derived epitopes in patients with pancreatic adenocarcinomas; our results suggested that $p53_{161}$, $hTERT_{461}$, $WT\text{-}1_{235}$, and $VEGFR2_{169}$ were the most suitable epitopes for cancer vaccine therapy.

Acknowledgments The authors thank Kazumi Fushimi, Maki Kawamura, Nami Nishiyama, and Mikiko Nakamura for their technical assistance.

Conflict of interest The authors do not have any conflict of interest.

References

1. Siegel R, Naishadham D, Jemal A (2012) Cancer statistics, 2012. CA Cancer J Clin 62:10–29
2. Hidalgo M (2010) Pancreatic cancer. N Engl J Med 362:1605–1617
3. Mellman I, Coukos G, Dranoff G (2011) Cancer immunotherapy comes of age. Nature 480:480–489
4. Arai J, Yasukawa M, Ohminami H, Kakimoto M, Hasegawa A, Fujita S (2001) Identification of human telomerase reverse transcriptase-derived peptides that induce HLA-A24-restricted anti-leukemia cytotoxic T lymphocytes. Blood 97:2903–2907
5. Ferries E, Connan F, Pages F, Gaston J, Hagnere AM, Vieillefond A, Thiounn N, Guillet J, Choppin J (2001) Identification of p53 peptides recognized by CD8(+) T lymphocytes from patients with bladder cancer. Hum Immunol 62:791–798
6. Fujie T, Tahara K, Tanaka F, Mori M, Takesako K, Akiyoshi T (1999) A MAGE-1-encoded HLA-A24-binding synthetic peptide induces specific anti-tumor cytotoxic T lymphocytes. Int J Cancer 80:169–172
7. Gomi S, Nakao M, Niiya F, Imamura Y, Kawano K, Nishizaka S, Hayashi A, Sobao Y, Oizumi K, Itoh K (1999) A cyclophilin B gene encodes antigenic epitopes recognized by HLA-A24-restricted and tumor-specific CTLs. J Immunol 163:4994–5004
8. Harashima N, Tanaka K, Sasatomi T, Shimizu K, Miyagi Y, Yamada A, Tamura M, Yamana H, Itoh K, Shichijo S (2001) Recognition of the Lck tyrosine kinase as a tumor antigen by cytotoxic T lymphocytes of cancer patients with distant metastases. Eur J Immunol 31:323–332
9. Hirohashi Y, Torigoe T, Maeda A, Nabeta Y, Kamiguchi K, Sato T, Yoda J, Ikeda H, Hirata K, Yamanaka N, Sato N (2002) An HLA-A24-restricted cytotoxic T lymphocyte epitope of a tumor-associated protein, survivin. Clin Cancer Res 8:1731–1739
10. Ishizaki H, Tsunoda T, Wada S, Yamauchi M, Shibuya M, Tahara H (2006) Inhibition of tumor growth with antiangiogenic cancer vaccine using epitope peptides derived from human vascular endothelial growth factor receptor 1. Clin Cancer Res 12:5841–5849
11. Kawano K, Gomi S, Tanaka K, Tsuda N, Kamura T, Itoh K, Yamada A (2000) Identification of a new endoplasmic reticulum-resident protein recognized by HLA-A24-restricted tumor-infiltrating lymphocytes of lung cancer. Cancer Res 60:3550–3558
12. Kikuchi M, Nakao M, Inoue Y, Matsunaga K, Shichijo S, Yamana H, Itoh K (1999) Identification of a SART-1-derived peptide capable of inducing HLA-A24-restricted and tumor-specific cytotoxic T lymphocytes. Int J Cancer 81:459–466
13. Nakao M, Shichijo S, Imaizumi T, Inoue Y, Matsunaga K, Yamada A, Kikuchi M, Tsuda N, Ohta K, Takamori S, Yamana H, Fujita H, Itoh K (2000) Identification of a gene coding for a new squamous cell carcinoma antigen recognized by the CTL. J Immunol 164:2565–2574
14. Nishizaka S, Gomi S, Harada K, Oizumi K, Itoh K, Shichijo S (2000) A new tumor-rejection antigen recognized by cytotoxic T lymphocytes infiltrating into a lung adenocarcinoma. Cancer Res 60:4830–4837
15. Ohminami H, Yasukawa M, Fujita S (2000) HLA class I-restricted lysis of leukemia cells by a CD8(+) cytotoxic T-lymphocyte clone specific for WT1 peptide. Blood 95:286–293
16. Tanaka F, Fujie T, Tahara K, Mori M, Takesako K, Sette A, Celis E, Akiyoshi T (1997) Induction of antitumor cytotoxic T lymphocytes with a MAGE-3-encoded synthetic peptide presented by human leukocytes antigen-A24. Cancer Res 57:4465–4468
17. Tanaka H, Tsunoda T, Nukaya I, Sette A, Matsuda K, Umano Y, Yamaue H, Takesako K, Tanimura H (2001) Mapping the HLA-A24-restricted T-cell epitope peptide from a tumour-associated antigen HER2/neu: possible immunotherapy for colorectal carcinomas. Br J Cancer 84:94–99
18. Umano Y, Tsunoda T, Tanaka H, Matsuda K, Yamaue H, Tanimura H (2001) Generation of cytotoxic T cell responses to an HLA-A24 restricted epitope peptide derived from wild-type p53. Br J Cancer 84:1052–1057
19. Wada S, Tsunoda T, Baba T, Primus FJ, Kuwano H, Shibuya M, Tahara H (2005) Rationale for antiangiogenic cancer therapy with vaccination using epitope peptides derived from human vascular endothelial growth factor receptor 2. Cancer Res 65:4939–4946
20. Yamada A, Kawano K, Koga M, Matsumoto T, Itoh K (2001) Multidrug resistance-associated protein 3 is a tumor rejection antigen recognized by HLA-A2402-restricted cytotoxic T lymphocytes. Cancer Res 61:6459–6466
21. Yang D, Nakao M, Shichijo S, Sasatomi T, Takasu H, Matsumoto H, Mori K, Hayashi A, Yamana H, Shirouzu K, Itoh K (1999) Identification of a gene coding for a protein possessing shared tumor epitopes capable of inducing HLA-A24-restricted cytotoxic T lymphocytes in cancer patients. Cancer Res 59:4056–4063
22. Novellino L, Castelli C, Parmiani G (2005) A listing of human tumor antigens recognized by T cells: March 2004 update. Cancer Immunol Immunother 54:187–207
23. Kaida M, Morita-Hoshi Y, Soeda A, Wakeda T, Yamaki Y, Kojima Y, Ueno H, Kondo S, Morizane C, Ikeda M, Okusaka T, Takaue Y, Heike Y (2011) Phase 1 trial of Wilms tumor 1 (WT1) peptide vaccine and gemcitabine combination therapy in patients with advanced pancreatic or biliary tract cancer. J Immunother 34:92–99
24. Miyazawa M, Ohsawa R, Tsunoda T, Hirono S, Kawai M, Tani M, Nakamura Y, Yamaue H (2010) Phase I clinical trial using peptide vaccine for human vascular endothelial growth factor receptor 2 in combination with gemcitabine for patients with advanced pancreatic cancer. Cancer Sci 101:433–439
25. Ikeda-Moore Y, Tomiyama H, Miwa K, Oka S, Iwamoto A, Kaneko Y, Takiguchi M (1997) Identification and characterization of multiple HLA-A24-restricted HIV-1 CTL epitopes: strong epitopes are derived from V regions of HIV-1. J Immunol 159:6242–6252
26. Kuzushima K, Hayashi N, Kimura H, Tsurumi T (2001) Efficient identification of HLA-A*2402-restricted cytomegalovirus-specific CD8(+) T-cell epitopes by a computer algorithm and an enzyme-linked immunospot assay. Blood 98:1872–1881
27. Oiso M, Eura M, Katsura F, Takiguchi M, Sobao Y, Masuyama K, Nakashima M, Itoh K, Ishikawa T (1999) A newly identified MAGE-3-derived epitope recognized by HLA-A24-restricted cytotoxic T lymphocytes. Int J Cancer 81:387–394
28. Sallusto F, Lenig D, Forster R, Lipp M, Lanzavecchia A (1999) Two subsets of memory T lymphocytes with distinct homing potentials and effector functions. Nature 401:708–712
29. Dodson LF, Hawkins WG, Goedegebuure P (2011) Potential targets for pancreatic cancer immunotherapeutics. Immunotherapy 3:517–537

30. Kantoff PW, Higano CS, Shore ND, Berger ER, Small EJ, Penson DF, Redfern CH, Ferrari AC, Dreicer R, Sims RB, Xu Y, Frohlich MW, Schellhammer PF (2010) Sipuleucel-T immunotherapy for castration-resistant prostate cancer. N Engl J Med 363:411–422
31. Cheever MA, Allison JP, Ferris AS, Finn OJ, Hastings BM, Hecht TT, Mellman I, Prindiville SA, Viner JL, Weiner LM, Matrisian LM (2009) The prioritization of cancer antigens: a national cancer institute pilot project for the acceleration of translational research. Clin Cancer Res 15:5323–5337
32. Schmitz-Winnenthal FH, Galindo-Escobedo LV, Rimoldi D, Geng W, Romero P, Koch M, Weitz J, Krempien R, Niethammer AG, Beckhove P, Buchler MW, Z'Graggen K (2007) Potential target antigens for immunotherapy in human pancreatic cancer. Cancer Lett 252:290–298
33. Singh P, Srinivasan R, Wig JD (2011) Major molecular markers in pancreatic ductal adenocarcinoma and their roles in screening, diagnosis, prognosis, and treatment. Pancreas 40:644–652
34. Suzuki K, Matsubara H (2011) Recent advances in p53 research and cancer treatment. J Biomed Biotechnol 2011:978312
35. Mizukoshi E, Nakamoto Y, Arai K, Yamashita T, Sakai A, Sakai Y, Kagaya T, Honda M, Kaneko S (2011) Comparative analysis of various tumor-associated antigen-specific t-cell responses in patients with hepatocellular carcinoma. Hepatology 53:1206–1216
36. Sakakura K, Chikamatsu K, Furuya N, Appella E, Whiteside TL, Deleo AB (2007) Toward the development of multi-epitope p53 cancer vaccines: an in vitro assessment of CD8(+) T cell responses to HLA class I-restricted wild-type sequence p53 peptides. Clin Immunol 125:43–51
37. Suehara N, Mizumoto K, Tanaka M, Niiyama H, Yokohata K, Tominaga Y, Shimura H, Muta T, Hamasaki N (1997) Telomerase activity in pancreatic juice differentiates ductal carcinoma from adenoma and pancreatitis. Clin Cancer Res 3:2479–2483
38. Bernhardt SL, Gjertsen MK, Trachsel S, Moller M, Eriksen JA, Meo M, Buanes T, Gaudernack G (2006) Telomerase peptide vaccination of patients with non-resectable pancreatic cancer: a dose escalating phase I/II study. Br J Cancer 95:1474–1482
39. Mizukoshi E, Nakamoto Y, Marukawa Y, Arai K, Yamashita T, Tsuji H, Kuzushima K, Takiguchi M, Kaneko S (2006) Cytotoxic T cell responses to human telomerase reverse transcriptase in patients with hepatocellular carcinoma. Hepatology 43:1284–1294
40. Shang XY, Chen HS, Zhang HG, Pang XW, Qiao H, Peng JR, Qin LL, Fei R, Mei MH, Leng XS, Gnjatic S, Ritter G, Simpson AJ, Old LJ, Chen WF (2004) The spontaneous CD8+ T-cell response to HLA-A2-restricted NY-ESO-1b peptide in hepatocellular carcinoma patients. Clin Cancer Res 10:6946–6955
41. van den Ancker W, Ruben JM, Westers TM, Wulandari D, Bontkes HJ, Hooijberg E, Stam AG, Santegoets SJ, Ossenkoppele GJ, de Gruijl T, van de Loosdrecht A (2013) Priming of PRAME- and WT1-specific CD8+ T cells in healthy donors but not in AML patients in complete remission: implications for immunotherapy. Oncoimmunology 2(4):e23971
42. Ho WY, Nguyen HN, Wolfl M, Kuball J, Greenberg PD (2006) In vitro methods for generating CD8+ T-cell clones for immunotherapy from the naïve repertoire. J Immunol Methods 310:40–52
43. Grivennikov SI, Greten FR, Karin M (2010) Immunity, inflammation, and cancer. Cell 140:883–899
44. Bellone G, Smirne C, Mauri FA, Tonel E, Carbone A, Buffolino A, Dughera L, Robecchi A, Pirisi M, Emanuelli G (2006) Cytokine expression profile in human pancreatic carcinoma cells and in surgical specimens: implications for survival. Cancer Immunol Immunother 55:684–698
45. Noguchi M, Mine T, Komatsu N, Suekane S, Moriya F, Matsuoka K, Yutani S, Shichijo S, Yamada A, Toh U, Kawano K, Azuma K, Uemura H, Okuno K, Matsumoto K, Yanagimoto H, Yamanaka R, Oka M, Todo S, Sasada T, Itoh K (2010) Assessment of immunological biomarkers in patients with advanced cancer treated by personalized peptide vaccination. Cancer Biol Ther 10:1266–1279
46. Laheru D, Lutz E, Burke J, Biedrzycki B, Onners B, Tartakovsky I, Nemunaitis J, Le D, Sugar E, Hege K, Jaffee E (2008) Allogenic granulocyte macrophage colony-stimulating factor-secreting tumor immunotherapy alone or in sequence with cyclophosphamide for metastatic pancreatic cancer: a pilot study of safety, feasibility, and immune activation. Cin Cancer Res 14:1455–1463

Diabetologia (2014) 57:878–890
DOI 10.1007/s00125-013-3149-9

ARTICLE

The effects of ezetimibe on non-alcoholic fatty liver disease and glucose metabolism: a randomised controlled trial

Yumie Takeshita · Toshinari Takamura · Masao Honda · Yuki Kita · Yoh Zen · Ken-ichiro Kato · Hirofumi Misu · Tsuguhito Ota · Mikiko Nakamura · Kazutoshi Yamada · Hajime Sunagozaka · Kuniaki Arai · Tatsuya Yamashita · Eishiro Mizukoshi · Shuichi Kaneko

Received: 11 October 2013 / Accepted: 15 November 2013 / Published online: 10 January 2014

Abstract

Aims/hypothesis The cholesterol absorption inhibitor ezetimibe has been shown to ameliorate non-alcoholic fatty liver disease (NAFLD) pathology in a single-armed clinical study and in experimental animal models. In this study, we investigated the efficacy of ezetimibe on NAFLD pathology in an open-label randomised controlled clinical trial.

Methods We had planned to enrol 80 patients in the trial, as we had estimated that, with this sample size, the study would have 90% power. The study intervention and enrolment were discontinued because of the higher proportion of adverse events (significant elevation in HbA_{1c}) in the ezetimibe group than in the control group. Thirty-two patients with NAFLD were enrolled and randomised (allocation by computer program). Ezetimibe (10 mg/day) was given to 17 patients with NAFLD for 6 months. The primary endpoint was change in serum aminotransferase level. Secondary outcomes were change in liver histology (12 control and 16 ezetimibe patients), insulin sensitivity including a hyperinsulinaemic–euglycaemic clamp study (ten control and 13 ezetimibe patients) and hepatic fatty acid composition (six control and nine ezetimibe patients). Hepatic gene expression profiling was completed in 15 patients using an Affymetrix gene chip. Patients and the physician in charge knew to which group the patient had been allocated, but people carrying out measurements or examinations were blinded to group.

Results Serum total cholesterol was significantly decreased in the ezetimibe group. The fibrosis stage and ballooning score were also significantly improved with ezetimibe treatment. However, ezetimibe treatment significantly increased HbA_{1c} and was associated with a significant increase in hepatic long-chain fatty acids. Hepatic gene expression analysis showed coordinate downregulation of genes involved in skeletal muscle development and cell adhesion molecules in the ezetimibe treatment group, suggesting a suppression of stellate cell development into myofibroblasts. Genes involved in the L-carnitine pathway were coordinately downregulated by ezetimibe treatment and those in the steroid metabolism pathway upregulated, suggestive of impaired oxidation of long-chain fatty acids.

Conclusions/interpretation Ezetimibe improved hepatic fibrosis but increased hepatic long-chain fatty acids and HbA_{1c} in patients with NAFLD. These findings shed light on previously unrecognised actions of ezetimibe that should be examined further in future studies.

Trial registration University Hospital Medical Information Network (UMIN) Clinical Trials Registry UMIN000005250.

Funding The study was funded by grants-in-aid from the Ministry of Education, Culture, Sports, Science and Technology, Japan, and research grants from MSD.

Keywords Ezetimibe · Fatty acid · Gene expression · Non-alcoholic fatty liver disease

Yumie Takeshita and Toshinari Takamura contributed equally to this work.

Electronic supplementary material The online version of this article (doi:10.1007/s00125-013-3149-9) contains peer-reviewed but unedited supplementary material, which is available to authorised users.

Y. Takeshita · T. Takamura (✉) · M. Honda · Y. Kita · K.-i. Kato · H. Misu · T. Ota · M. Nakamura · K. Yamada · H. Sunagozaka · K. Arai · T. Yamashita · E. Mizukoshi · S. Kaneko
Department of Disease Control and Homeostasis, Kanazawa University Graduate School of Medical Sciences,
13-1 Takara-machi, Kanazawa, Ishikawa 920-8641, Japan
e-mail: ttakamura@m-kanazawa.jp

Y. Zen
Histopathology Section, Institute of Liver Studies, King's College Hospital, London, UK

Abbreviations

ALT	Alanine aminotransferase
H-IR	Hepatic insulin resistance index
hsCRP	High-sensitivity C-reactive protein
ICG15	Indocyanine green retention rate at 15 min after venous administration
LXR	Liver-X-receptor
MCR	Glucose metabolic clearance rate
miR	MicroRNA
NAFLD	Non-alcoholic fatty liver disease
NAS	NAFLD activity score
NASH	Non-alcoholic steatohepatitis
NPC1L1	Niemann–Pick C1-like 1
PAI-1	Plasminogen activator inhibitor-1
RLP-C	Remnant-like particle cholesterol
sdLDL	Small dense LDL
SREBP	Sterol regulatory element binding protein
QUICKI	Quantitative insulin sensitivity check index

Introduction

Multiple metabolic disorders, such as diabetes [1], insulin resistance and dyslipidaemia [2], are associated with non-alcoholic fatty liver disease (NAFLD), ranging from simple fatty liver to non-alcoholic steatohepatitis (NASH). Steatosis of the liver is closely associated with insulin resistance. However, the toxic lipids are not intrahepatic triacylglycerols but, rather, it is non-esterified cholesterol [3, 4] and some NEFA [5] that contribute to inflammation and insulin resistance in hepatocytes.

The level of cholesterol is tightly regulated by endogenous synthesis in the liver and dietary absorption/biliary reabsorption in the small intestine. Niemann–Pick C1-like 1 (NPC1L1) plays a pivotal role in cholesterol incorporation in enterocytes [6]. Ezetimibe, a potent inhibitor of cholesterol absorption, inhibits NPC1L1-dependent cholesterol transport at the brush border of the intestine and the liver [6]. This suggests that ezetimibe ameliorates toxic-lipid-induced inflammation and insulin resistance by inhibiting cholesterol absorption. Indeed, ezetimibe improves liver steatosis and insulin resistance in mice [7] and Zucker obese fatty rats [8], although the beneficial effects of ezetimibe are observed only when the animals are fed a high-fat diet. Ezetimibe can also ameliorate liver pathology in patients with NAFLD [9, 10]; however, these studies lack a control group, which precludes meaningful conclusions as liver pathology can improve over the natural course of the disease or with tight glycaemic control in some NAFLD patients [1]. In the present study, we investigated the efficacy of ezetimibe treatment in patients with NAFLD for 6 months in an open-label randomised control study by examining liver pathology, as well as hepatic enzymes, glucose metabolism, hepatic fatty acid composition and hepatic gene expression profiles.

Methods

Patient selection Study staff recruited participants from outpatients at Kanazawa University Hospital, Ishikawa, Japan. Patients were recruited from April 2008 to August 2010, with follow-up visits during the 6 months thereafter. The study lasted from April 2008 to February 2011.

The inclusion criterion was a biopsy consistent with the diagnosis of NAFLD. Exclusion criteria included hepatic virus infections (hepatitis C virus [HCV] RNA–PCR-positive, hepatitis B and C, cytomegalovirus and Epstein–Barr virus), autoimmune hepatitis, primary biliary cirrhosis, sclerosing cholangitis, haemochromatosis, α_1-antitrypsin deficiency, Wilson's disease, history of parenteral nutrition and use of drugs known to induce steatosis (e.g. valproate, amiodarone and prednisone) or hepatic injury caused by substance abuse and/or the current or past consumption of more than 20 g of alcohol daily. None of the patients had any clinical evidence of hepatic decompensation, such as hepatic encephalopathy, ascites, variceal bleeding or an elevated serum bilirubin level more than twofold the upper normal limit.

A random allocation sequence was computer-generated elsewhere and assigned participants in a 1:1 ratio to treatment with ezetimibe or to the control group. All patients and responsible guardians underwent an hour of nutritional counselling by an experienced dietitian before starting the 6 month treatment period. The experienced dietitians were unaware of the study assignments. In addition, all patients were given a standard energy diet (125.5 kJ/kg per day; carbohydrate 50–60%, fat 20–30%, protein 15–20%) and exercise (5–6 metabolic equivalent estimations for 30 min daily) counselling before the study. Patients remained on stable doses of medications for the duration of the study. The patients in the ezetimibe group received generic ezetimibe (10 mg/day; Zetia, [Merck, Whitehouse Station, NJ, USA]) for 6 months.

The study was conducted with the approval of the Ethics Committee of Kanazawa University Hospital, Ishikawa, Japan, in accordance with the Declaration of Helsinki. Written informed consent was obtained from all individuals before enrolment. This trial is registered with the University Hospital Medical Information Network (UMIN) (Clinical Trials Registry, no. UMIN000005250).

Primary and secondary outcomes The primary endpoint was change in serum alanine aminotransferase (ALT) level at month 6 from baseline. Secondary outcomes included changes in the histological findings for NAFLD, hepatic gene expression profiling, fatty acid compositions of plasma and liver biopsy samples, lipid profiles, insulin resistance and

anthropometric measures, as well as assessment of ezetimibe safety. We had planned to enrol 80 patients in the trial, as we had estimated that with this sample size, the study would have 90% power at an α (two-tailed) value of 0.05 showing a 50% decrease of serum ALT values with 6 months of pioglitazone therapy on the basis of a previous study [11]. At the time of adverse event analyses, 32 of the targeted 80 patients had been randomly assigned and were included in the safety analyses.

Data collection Clinical information, including age, sex and body measurements, was obtained for each patient. Venous blood samples were obtained after the patients had fasted overnight (12 h) and were used to evaluate blood chemistry. Insulin resistance was estimated by HOMA-IR, calculated as [fasting insulin (pmol/l) × fasting glucose (mmol/l)]/22.5 [12] and insulin sensitivity was estimated as the quantitative insulin sensitivity check index (QUICKI)[13]. The adipose tissue insulin resistance index (adipose IR) was calculated as fasting NEFA (mmol/l)×fasting insulin (pmol/l) [14–16]. The indocyanine green retention rate at 15 min after venous administration (ICG15) was assessed using standard laboratory techniques before and after treatment. Serum fatty acids were measured with a gas chromatograph (Shimizu GC 17A, Kypto, Japan) at SRL (Tokyo, Japan).

Evaluation of insulin sensitivity derived from an OGTT After an overnight fast (10–12 h), a 75 g OGTT was performed at 08:30 hours. The OGTT-derived index of beta cell function, the insulinogenic index, computed as the suprabasal serum insulin increment divided by the corresponding plasma glucose increment in the first 30 min (ΔI30/ΔG30) [15, 17, 18] was calculated. From the OGTT data, the Matsuda index [19] was calculated. The hepatic insulin resistance index (H-IR) was calculated as the product of the total AUCs for glucose and insulin during the first 30 min of the OGTT (glucose 0–30 [AUC] [mmol/l]×insulin 0–30 [AUC] [pmol/l]). Skeletal muscle insulin sensitivity can be calculated as the rate of decline in plasma glucose concentration divided by plasma insulin concentration, as follows. Muscle insulin sensitivity index=dG/dt/mean plasma insulin concentration, where dG/dt is the rate of decline in plasma glucose concentration and is calculated as the slope of the least square fit to the decline in plasma glucose concentration from peak to nadir [20]. See the electronic supplementary material (ESM) for further details.

Evaluation of insulin sensitivity derived from the euglycaemic insulin clamp Insulin sensitivity in 23 of the 31 patients (10 control and 13 ezetimibe patients) was also evaluated in a hyperinsulinaemic–euglycaemic clamp study [21]. Patients did not receive any medication on the morning of the examination. At ~09:00 hours, after an overnight fast of at least 10 h, an intravenous catheter was placed in an antecubital vein in each individual for infusion, while a second catheter was placed in the contralateral hand for blood sampling. The euglycaemic–hyperinsulinaemic clamp technique was performed using an artificial pancreas (model STG-22; Nikkiso, Tokyo, Japan), as described previously [22]. See ESM for further details. The mean glucose metabolic clearance rate (MCR) in healthy individuals (n=9; age, 26.60± 2.9 years; body mass index, 22.3±2.1 kg/m^2) was 13.5± 3.4 mg kg^{-1} min^{-1} [2].

Liver biopsy pathology A single pathologist, who was blinded to the clinical information and the order in which the biopsies were obtained, analysed all biopsies twice and at separate times. The sections were cut from a paraffin block and stained with haematoxylin and eosin, Azan–Mallory and silver reticulin impregnation. The biopsied tissues were scored for steatosis (from 0 to 3), stage (from 1 to 4) and grade (from 1 to 3) as described [2], according to the standard criteria for grading and staging of NASH proposed by Brunt et al [23]. The NAFLD activity score (NAS) was calculated as the unweighted sum of the scores for steatosis (0–3), lobular inflammation (0–3) and ballooning (0–2), as reported by Kleiner et al [24].

Gene expression analysis of liver biopsied samples Gene expression profiling was performed in samples from nine patients in the ezetimibe group and six in the control group. Liver tissue RNA was isolated using the RNeasy Mini kit (QIAGEN, Tokyo, Japan) according to the manufacturer's instructions. See ESM for further details. Data files (CEL) were obtained using the GeneChip Operating Software 1.4 (Affymetrix). Genechip data analysis was performed using BRB-Array Tools (http://linus.nci.nih.gov/BRB-ArrayTools.html). The data were log-transformed ($\log_{10}$), normalised and centred. To identify genetic variants, paired t tests were performed to define p values <0.05 and fold change>1.5. Pathway analysis was performed using MetaCore (GeneGo, St Joseph, MI, USA). Functional ontology enrichment analysis was performed to compare the gene ontology (GO) process distribution of differentially expressed genes ($p < 0.01$).

Fatty acid composition of liver Aliquots (0.2 mg) of liver samples snap-frozen by liquid nitrogen were homogenised in 1 ml normal NaCl solution (NaCl 154 mmol/l). Briefly, fatty acids were extracted by using pentadecanoic acid, and saponified with alkaline reagent (0.5 mmol/l KOH/ CH_3OH). The fatty acid methyl esters were analysed in a gas chromatograph (Shimadzu GC-2014 AF/SPL; Shimadzu Corporation, Kyoto, Japan) equipped with a flame ionisation detector and an auto injector. See ESM for further details. Mass spectra were analysed using GC solution (v. 2.3) software (Shimadzu Corporation, Kyoto, Japan, www.shimadzu.com). The changes in hepatic fatty acid composition are expressed as 10^{-4} mg/mg liver.

Statistical analysis Data are expressed as mean ± one standard error, unless indicated otherwise. The Statistical Package for the Social Sciences (SPSS; version 11.0; Chicago, IL, USA) was used for the statistical analyses. For univariate comparisons between the patient groups, Student's *t* test or Mann–Whitney's *U* test was used, as appropriate, followed by the Bonferroni multiple-comparison test. A value of $p < 0.05$ was considered to indicate statistical significance.

Results

Enrolment and discontinuation The data and safety monitoring board recommended that the study intervention and enrolment be discontinued because of the higher proportion of adverse events (significant elevation in HbA_{1c}) in the ezetimibe group than in the control group. At the time of adverse event analyses, 32 of the targeted 80 patients had been randomly assigned and were included in the safety analyses. In our open-label trial, 32 patients with NAFLD were enrolled. They were randomised to treatment with ezetimibe ($n=17$) or a control ($n=15$) with no significant clinical differences in variables between the groups. Of the 32 randomly assigned patients, 31 had completed the 6 month intervention period; one patient dropped out of the study. One case in the control group withdrew consent after randomisation and before intervention (ESM Fig. 1). The patient who withdrew was excluded from analysis because he did not start his course of treatment. Two analyses were conducted in the remaining patients. In the intention-to-treat analysis (ESM Tables 1 and 2), measures that were missing for participants who discontinued the study were replaced with baseline measures. In the second analysis, the only data included were from participants who completed the study to the end of the 6 month follow-up period. We performed a completed case analysis because there were few dropouts unrelated to baseline values or to their response.

Patient characteristics The 31 study patients (mean age 52.7±2.1 years; mean BMI 29.2±1.0) included 14 randomised to the control group and 17 to the ezetimibe group (ESM Table 3).

At baseline, the characteristics of patients in the ezetimibe and control groups were comparable except for the waist circumference ($p=0.085$) and the Matsuda index ($p=0.060$). The histological features of the liver are summarised in Table 1. At baseline, neither the severity of the individual histological features nor the proportion of patients distributed in the three NAS categories was significantly different between the two groups. All 31 participants agreed to complete the follow-up venous blood samples including OGTT. The ICG15 was conducted in 24 patients (ten control and 14 ezetimibe patients).

Changes in laboratory variables The primary study outcome, serum alanine aminotransferase levels, did not change after ezetimibe treatment (Table 2).

After 6 months of ezetimibe treatment, systolic blood pressure, HbA_{1c}, glycated albumin, and lathosterol were significantly increased, while total cholesterol levels, campesterol, sitosterol and ferritin were significantly decreased. In contrast, body weight, BMI, fasting plasma glucose, plasma γ-glutamyltransferase, triacylglycerols, HDL-cholesterol, small dense LDL (sdLDL), remnant-like particle cholesterol (RLP-C), type IV collagen 7 s levels, NEFA, total bile acid, high-sensitivity C-reactive protein (hsCRP), adiponectin, TNF-α, plasminogen activator inhibitor-1 (PAI-1), 8-isoprostanes and ICG15 did not change after ezetimibe treatment (Table 2). Adipose IR tended to increase in the ezetimibe group (from 88.1±25.5 to 107.5±25.5, $p=0.070$), but not in the control group.

When changes in the groups were compared, the ezetimibe group, but not the control group, had a significant decrease in total cholesterol (ezetimibe, −0.49±0.19 vs control, 0.06±0.14 mmol/l; $p=0.037$), whereas the ezetimibe group, but not control group, showed a significant elevation in HbA_{1c} (ezetimibe, 0.46±0.12% [4.95±1.28 mmol/mol] vs control, 0.08±0.13% [0.78±1.46 mmol/mol]; $p=0.041$). Also, there were significant differences between the groups in cholesterol and HbA_{1c} levels at 6 months. The multiple-comparison

Table 1 Histological characteristics of the livers of patients who completed the study at baseline and 6 months

Variable	Control		p^a	Ezetimibe		p^a	p^b
	Before	After		Before	After		
Steatosis	1.42±0.15	1.17±0.17	0.082	1.56±0.18	1.31±0.15	0.300	0.989
Stage	1.71±0.40	1.71±0.39	1.000	1.75±0.28	1.53±0.26	0.048	0.163
Grade	0.88±0.28	0.79±0.26	0.339	0.84±0.21	0.72±0.15	0.362	0.628
Acinar inflammation	0.88±0.20	0.83±0.20	0.674	1.00±0.13	0.97±0.13	0.751	0.060
Portal inflammation	0.67±0.19	0.71±0.13	0.795	0.44±0.16	0.56±0.16	0.333	0.941
Ballooning	0.58±0.23	0.58±0.23	1.000	0.69±0.20	0.41±0.15	0.045	0.677
NAFLD activity score	3.25±0.53	2.82±0.59	0.139	3.71±0.50	3.06±0.45	0.185	0.705

Data are expressed as the means ± SE

[a] p value for the intergroup comparison (baseline vs 6 month)

[b] p value for the intergroup comparison (changes from baseline between groups)

Table 2 Laboratory values, insulin sensitivity and insulin resistance derived from the euglycaemic insulin clamps and OGTTs of patients who completed the study at baseline and 6 months

Variable	Control			Ezetimibe			
	Before	After	p^a	Before	After	p^a	p^b
Male/female	9/5			11/6			0.232
Age (years)	55.5±3.0			50.4±2.9			
Body weight (kg)	74.4±6.2	73.0±5.6	0.144	81.5±4.6	80.1±4.2	0.367	0.983
BMI (kg/m^2)	27.7±1.7	27.3±1.5	0.172	30.5±1.2	30.0±1.1	0.383	0.999
Waist circumference (cm)	93.1±2.7	92.6±3.4	0.709	99.9±2.5	100.0±2.6	0.956	0.713
Systolic blood pressure (mmHg)	125.2±3.9	126.4±4.9	0.771	124.0±2.4	130.7±2.8	0.048	0.269
Fasting plasma glucose (mmol/l)	7.15±0.63	6.52±0.40	0.240	6.62±0.30	6.87±0.34	0.411	0.131
HbA_{1c} (%)	5.9±0.2	6.0±0.2	0.603	6.1±0.2	6.5±0.2	0.001	0.041
HbA_{1c} (mmol/mol)	40.8±2.2	41.6±2.6	0.603	43.0±2.6	48.0±2.3	0.001	0.041
Hepaplastin test (%)	115.9±5.8	117.1±6.4	0.624	113.7±4.6	111.8±3.7	0.583	0.459
Glycated albumin (%)	15.9±0.8	16.2±1.0	0.397	15.7±0.5	16.8±0.5	0.014	0.196
Serum aspartate aminotransferase (μkat/l)	31.1±4.4	30.3±3.0	0.780	41.8±6.7	33.7±4.1	0.252	0.365
Serum ALT (μkat/l)	37.9±6.8	38.0±4.5	0.978	53.2±8.6	49.3±6.5	0.683	0.723
Plasma γ-glutamyltransferase (μkat/l)	74.9±27.8	65.8±19.5	0.345	71.4±23.4	60.5±16.1	0.220	0.892
Total cholesterol (mmol/l)	5.14±0.21	5.20±0.18	0.672	5.14±0.20	4.65±0.17	0.024	0.037
Triacylglycerols (mmol/l)	1.34±0.12	1.17±0.12	0.105	1.43±0.11	1.46±0.13	0.857	0.303
HDL-C (mmol/l)	1.40±0.08	1.45±0.06	0.914	1.36±0.08	1.36±0.06	0.942	0.903
sdLDL (mmol/l)	0.52±0.07	0.54±0.07	0.782	0.61±0.10	0.50±0.06	0.201	0.251
RLP-C (mmol/l)	0.13±0.01	0.11±0.01	0.163	0.12±0.01	0.11±0.01	0.601	0.365
Lathosterol×10^{-3} (μmol/l)	2.27±0.43	2.85±0.52	0.001	3.52±0.52	5.01±0.67	<0.001	0.018
Campesterol×10^{-3} (μmol/l)	4.32±0.65	6.20±0.68	0.004	3.78±0.42	2.49±0.30	0.007	<0.001
Sitosterol×10^{-3} (μmol/l)	3.04±0.47	3.89±0.39	0.079	2.73±0.28	1.81±0.19	0.004	0.002
Ferritin (pmol/l)	412.1±85.6	235.3±47.0	0.009	395.7±81.3	247.8±56.8	0.005	0.689
Type IV collagen 7 s (μg/l)	4.52±0.48	4.42±0.45	0.622	4.23±0.23	4.33±0.20	0.592	0.465
NEFA (mmol/l)	0.50±0.09	0.63±0.06	0.160	0.51±0.05	0.57±0.03	0.835	0.447
Total bile acid (μmol/l)	12.5±8.0	8.8±5.2	0.214	5.0±0.7	4.8±1.3	0.893	0.267
hsCRP×10^{-3} (μg/ml)	0.12±0.02	0.09±0.02	0.050	0.14±0.04	0.13±0.04	0.886	0.767
Adiponectin (μg/ml)	4.0±0.5	4.6±0.8	0.114	3.0±0.6	3.3±0.6	0.299	0.670
TNF-α ×10^{-5} (pmol/ml)	10.4±2.3	15.6±8.1	0.094	8.1±0.6	30.0±12.7	0.183	0.084
Leptin×10^{-3} (μg/l)	8.1±1.0	9.7±1.3	0.044	10.8±1.4	12.4±1.5	0.085	0.982
PAI-1 (pmol/l)	400.0±44.2	436.5±44.2	0.401	550.0±71.2	488.5±67.3	0.217	0.136
8-Isoprostanes (pmol/mmol creatinine)	76.9±14.3	57.0±8.0	0.147	56.5±6.6	68.0±7.7	0.092	0.031
ICG15 (%)	8.7±2.4	8.5±2.0	0.662	7.7±1.7	7.7±1.5	0.984	0.796
HOMA-IR	10.1±6.5	5.0±2.1	0.471	9.5±2.6	9.3±2.2	0.839	0.479
QUICKI	0.32±0.01	0.33±0.01	0.443	0.30±0.01	0.30±0.01	0.984	0.019
Adipose IR	55.8±15.5	78.8±31.7	0.441	88.1±25.5	107.5±25.5	0.070	0.099
Insulinogenic index	0.43±0.09	0.53±0.11	0.307	0.41±0.08	0.35±0.09	0.501	0.765
H-IR×10^6	1.82±0.46	2.29±0.44	0.568	2.29±0.33	2.66±0.41	0.221	0.796
Matsuda index	3.03±0.45	3.35±0.49	0.368	1.99±0.28	2.01±0.29	0.895	0.013
Muscle insulin sensitivity	0.039±0.006	0.058±0.016	0.210	0.036±0.005	0.034±0.004	0.560	0.067
MCR	4.86±0.50	4.36±0.45	0.174	4.70±0.31	4.80±0.35	0.827	0.352

Data are expressed as means ± SE

[a] p value for the intergroup comparison (baseline vs 6 month)

[b] p value for the intergroup comparison (changes from baseline between groups)

HDL-C, HDL-cholesterol

Table 3 Signalling pathway gene expression changes in the ezetimibe group

Pathway	Gene symbol	Gene name	Affy ID	Up or down	Function
Development_skeletal muscle development	*VEGFA*	Vascular endothelial growth factor A	210512_s_at	Down	Angiogenesis
	ACTA2	Actin, α2, smooth muscle, aorta1	200974_at	Down	Cytoskeleton and cell attachment
	TCF3	Transcription factor 3	209153_s_at	Down	Differentiation
	TTN	Titin	1557994_at	Down	Abundant protein of striated muscle
	TPM2	Tropomyosin 2	204083_s_at	Down	Actin filament binding protein
	MYH11	Myosin, heavy chain 11, smooth muscle	201496_x_at	Down	Smooth muscle myosin
Immune response_phagocytosis	*FYB*	FYN-binding protein	205285_s_at	Up	Platelet activation and IL2 expression
	FCGR3A	Fc fragment of IgG, low affinity IIIA	204006_s_at	Up	ADCC and phagocytosis
	LCP2	Lymphocyte cytosolic protein 2	244251_at	Up	T cell antigen receptor mediated signalling
	CLEC7A	C-type lectin domain family 7, member A	221698_s_at	Up	T cell proliferation
	MSR1	Macrophage scavenger receptor 1	214770_at	Up	Macrophage-associated processes
	FCGR2A	Fc fragment of IgG, low affinity IIA	1565673_at	Up	Promotes phagocytosis
	PRKCB	Protein kinase C, β	209685_s_at	Up	B cell activation, apoptosis induction
	PLCB4	Phospholipase C, β4	240728_at	Up	Inflammation, cell growth, signalling and death
Cell adhesion_integrin priming	*GNA12*	G protein α12	221737_at	Down	Cytoskeletal rearrangement
	ITGB3	Integrin, β3	204628_s_at	Down	Ubiquitously expressed adhesion molecules
	PIK3R2	Phosphoinositide-3-kinase, regulatory subunit 2	229392_s_at	Down	Diverse range of cell functions
Cell adhesion_cadherins	*PTPRF*	Protein tyrosine phosphatase, receptor type, F	200636_s_at	Down	Cell adhesion receptor
	BTRC	β-Transducin repeat containing E3 ubiquitin protein ligase	222374_at	Down	Substrate recognition component of a SCF E3 ubiquitin-protein ligase complex
	CDHR2	Cadherin-related family member 2	220186_s_at	Down	Contact inhibition at the lateral surface of epithelial cells
	SKI	V-ski sarcoma viral oncogene homologue	229265_at	Down	Repressor of TGF-β signalling
	MLLT4	Myeloid/lymphoid or mixed-lineage leukaemia	214939_x_at	Down	Belongs to an adhesion system
	VLDLR	Very low density lipoprotein receptor	209822_s_at	Down	Binds VLDL and transports it into cells by endocytosis
O-Hexadecanoyl-L-carnitine pathway	*TUBB2B*	Tubulin, β 2B class IIB	209372_x_at	Down	Major component of microtubules
	TUBB2A	Tubulin, β2A class IIA	209372_x_at	Down	Major component of microtubules
	PLCE1	Phospholipase C, epsilon 1	205112_at	Down	Hydrolyses phospholipids into fatty acids and other lipophilic molecules
	CPT1B	Carnitine palmitoyltransferase 1B (muscle)	210070_s_at	Down	Rate-controlling enzyme of the long-chain fatty acid β-oxidation pathway
	CPT1A	Carnitine palmitoyltransferase 1A (liver)	203634_s_at	Down	Carnitine-dependent transport across the mitochondrial inner membrane
	NR1H4	Nuclear receptor subfamily 1, group H, member 4	243800_at	Down	Involved in bile acid synthesis and transport.
GalNAcbeta1-3Gal pathway	*PLCB4*	Phospholipase C, β4	240728_at	Up	Formation of inositol 1,4,5-trisphosphate and diacylglycerol
Steroid metabolism_cholesterol biosynthesis	*CYP51A1*	Cytochrome P450, family 51, subfamily A, polypeptide 1	216607_s_at	Up	Transforms lanosterol
	SREBF2	Sterol regulatory element binding transcription factor 2	242748_at	Up	Transcriptional activator required for lipid homeostasis
	SQLE	Squalene epoxidase	209218_at	Up	Catalyses the first oxygenation step in sterol biosynthesis

Table 3 (continued)

Pathway	Gene symbol	Gene name	Affy ID	Up or down	Function
	SC5DL	Sterol-C5-desaturase-like	215064_at	Up	Catalyses the conversion of lathosterol into 7-dehydrocholesterol
	HMGCS1	3-Hydroxy-3-methylglutaryl-CoA synthase 1	205822_s_at	Up	Condenses acetyl-CoA with acetoacetyl-CoA to form HMG-CoA

Bonferroni test revealed highly significant differences in the changes in total cholesterol ($p = 0.037$) and HbA_{1c} ($p = 0.040$) between the ezetimibe and control groups.

Increased concentrations of the cholesterol synthesis markers lathosterol (ezetimibe, 1.49±0.32 nmol/l vs control, 0.58±0.14 nmol/l; $p = 0.018$) and decreased concentrations of the cholesterol absorption markers campesterol (ezetimibe, −1.28±0.41 nmol/l vs control, 1.88±0.54 nmol/l, $p = 0.000$) and sitosterol (ezetimibe, −0.91±0.27 nmol/l vs control, 0.85± 0.45 nmol/l; $p = 0.002$) were observed on treatment. The ezetimibe group had an increase, whereas the control group had a decrease, in the level of 8-isoprostanes (ezetimibe, 11.6± 6.4 pmol/mmol creatinine vs control, −19.9±12.9 pmol/mmol creatinine; $p = 0.031$).

When changes between groups were compared, the ezetimibe group had a greater decrease in the Matsuda index (ezetimibe=−0.78±0.57 vs control=−1.35±0.55, $p = 0.013$), QUICKI (ezetimibe= −0.02±0.01 vs control=0.03±0.0, $p = 0.019$), and muscle insulin sensitivity (ezetimibe= −0.002±0.004 vs control=0.019±0.014, $p = 0.067$) than the control group.

Changes in liver histology Twenty-eight of 31 participants, 16 in the ezetimibe group and 12 in the control group, agreed to complete the follow-up and undergo a liver biopsy at 6 months, allowing for complete case analysis of the data (Table 1). After 6 months, the changes in staging score (from 1.75±0.28 to 1.53±0.26) and ballooning score (from 0.69± 0.20 to 0.41±0.15) were significantly improved in the ezetimibe group compared with the control group, whereas the scores of steatosis, lobular inflammation and NAS were not significantly changed in either group. The degree of all of these histological features was not significantly different between the two groups (Table 1).

Serial changes in liver gene with ezetimibe treatment Gene expression profiling was conducted in samples from nine patients in the ezetimibe group and six in the control group (ESM Table 4). In the ezetimibe group, 434 genes were upregulated and 410 genes downregulated, while in the control group, 643 genes were upregulated and 367 genes downregulated. Pathway analysis of the process network of differentially expressed genes showed coordinate downregulation of genes involved in skeletal muscle development and cell adhesion molecules in the ezetimibe group, suggesting a suppression of stellate cell development into myofibroblasts (Table 3). In addition, ezetimibe activated the immune response pathway. In contrast, genes involved in skeletal muscle development were upregulated and those in the immune response downregulated in the control group (Table 4). Pathway analysis of the metabolic network also revealed decreased L-carnitine pathway and increased steroid metabolism with ezetimibe treatment, but decreased CoA biosynthesis and increased glycerol 3-phosphate pathway in the control group (ESM Fig. 2).

Changes in plasma fatty acid composition and fatty acid composition extracted from liver tissue The changes in plasma fatty acid composition are shown in Table 5. Compared with baseline levels, only eicosatrienoic acid was significantly increased in the ezetimibe group.

Fatty acid composition in extracted liver tissue was available for 16 NAFLD patients treated with ezetimibe and 12 controls (Table 6). Ezetimibe treatment for 6 months significantly and markedly increased hepatic lauric, myristic, palmitic, palmitoleic, margaric and stearic acids compared with the control group. The changes in hepatic fatty acid composition did not correlate with the changes in serum fatty acid composition before and after ezetimibe treatment (ESM Table 5).

Discussion

This is the first report of the efficacy of ezetimibe treatment on liver pathology in patients with NAFLD in an open-label randomised controlled trial. Treatment with 10 mg/day ezetimibe for 6 months did not alter the primary study outcome, serum aminotransferase levels. Ezetimibe significantly decreased serum cholesterol levels and cholesterol absorption markers as expected, whereas, in contrast to previous reports, ezetimibe treatment did not decrease serum levels of triacylglycerol. Our initial hypothesis was that ezetimibe treatment ameliorates liver pathology by inhibiting the absorption of toxic lipids such as oxidised cholesterol and palmitate. In our animal model, cholesterol feeding to mice increased not

Table 4 Signalling pathway gene expression changes in the control group

Pathway	Gene symbol	Gene name	Affy ID	Up or down	Function
Muscle contraction	*MYH11*	Myosin, heavy chain 11, smooth muscle	201497_x_at	Up	Smooth muscle myosin
	CALM1	Calmodulin 1	241619_at	Up	Ion channels and other proteins by Ca^{2+}
	KCNJ15	Potassium inwardly-rectifying channel, subfamily J, member 15	211806_s_at	Up	Integral membrane protein, inward-rectifier type potassium channel
	SRI	Sorcin	208920_at	Up	Modulates excitation–contraction coupling in the heart
	ACTA2	Actin, α2, smooth muscle, aorta	215787_at	Up	Cell motility, structure and integrity
	TTN	Titin	1557994_at	Up	Abundant protein of striated muscle
	EDNRA	Endothelin receptor type A	204463_s_at	Up	Receptor for endothelin-1
	TPM2	Tropomyosin 2	204083_s_at	Up	Actin filament binding protein
	CRYAB	Crystallin, αB	209283_at	Up	Transparency and refractive index of the lens
Development_skeletal muscle development	*GTF2IRD1*	GTF2I repeat domain containing 1	218412_s_at	Up	Transcription regulator involved in cell-cycle progression, skeletal muscle differentiation
	ADAM12	ADAM metallopeptidase domain 12	213790_at	Up	Skeletal muscle regeneration
	MAP1B	Microtubule-associated protein 1B	226084_at	Up	Facilitates tyrosination of α-tubulin in neuronal microtubules
	MYOM1	Myomesin 1	205610_at	Up	Major component of the vertebrate myofibrillar M band
Cell cycle_G1-S growth factor regulation	*DACH1*	Dachshund homologue 1	205472_s_at	Up	Transcription factor that is involved in regulation of organogenesis
	FOXN3	Forkhead box N3	229652_s_at	Up	Transcriptional repressor, DNA damage-inducible cell cycle arrests
	TGFB2	Transforming growth factor, β2	228121_at	Up	Suppressive effects on interleukin-2 dependent T cell growth
	PIK3CD	Phosphatidylinositol-4,5-bisphosphate 3-kinase, catalytic subunit delta	203879_at	Up	Generate PIP3, recruiting PH domain-containing proteins to the membrane
	EGFR	Epidermal growth factor receptor	1565484_x_at	Up	Antagonist of EGF action
	CCNA2	Cyclin A2	203418_at	Up	Control of the cell cycle at the G1/S and the G2/M transitions
	AKT3	v-Akt murine thymoma viral oncogene homologue 3	219393_s_at	Up	Metabolism, proliferation, cell survival, growth and angiogenesis
	PRKD1	Protein kinase D1	205880_at	Up	Converts transient DAG signals into prolonged physiological effects
Regulation of metabolism_	*INSR*	Insulin receptor	226450_at	Down	Pleiotropic actions of insulin
Bile acid regulation of lipid metabolism and	*SLC27A5*	Solute carrier family 27, member 5	219733_s_at	Down	Bile acid metabolism
Negative FXR-dependent regulation of bile acids concentration	*MBTPS2*	Membrane-bound transcription factor peptidase	1554604_at	Down	Intramembrane proteolysis of SREBPs
	PIK3R3	Phosphoinositide-3-kinase, regulatory subunit 3	202743_at	Down	During insulin stimulation, it also binds to IRS-1
	MTTP	Microsomal triacylglycerol transfer protein	205675_at	Down	Catalyses the transport of triglyceride, cholesteryl ester, and phospholipid
	PPARA	Peroxisome proliferator-activated receptor α	226978_at	Down	Ligand-activated transcription factor
	CYP7A1	Cytochrome P450, family 7, subfamily A	207406_at	Down	Catalyses cholesterol catabolism and bile acid biosynthesis
	FOXA3	Forkhead box A3	228463_at	Down	Transcription factor

Table 4 (continued)

Pathway	Gene symbol	Gene name	Affy ID	Up or down	Function
Immune response_phagosome in antigen presentation	*HLA-B*	Major histocompatibility complex, class I, B	211911_x_at	Down	Foreign antigens to the immune system
	CD14	CD14 molecule	201743_at	Down	Mediates the innate immune response to bacterial lipopolysaccharide
	LBP	Lipopolysaccharide binding protein	211652_s_at	Down	Binds to the lipid A moiety of bacterial lipopolysaccharides
	CTSS	Cathepsin S	202901_x_at	Down	Thiol protease
	DERL1	Derlin 1	222543_at	Down	Functional component of endoplasmic reticulum-associated degradation
	CFL2	Cofilin 2	224352_s_at	Down	Reversibly controls actin polymerisation and depolymerisation
	PAK1	p21 protein (Cdc42/Rac)-activated kinase 1	230100_x_at	Down	Activated kinase acts on a variety of targets
Vitamin, mediator and cofactor	*SLC1A2*	Solute carrier family 1, member 2	1558009_at	Down	Transports L-glutamate and also L- and D-aspartate
Metabolism_CoA biosynthesis and transport	*PANK3*	Pantothenate kinase 3	218433_at	Down	Physiological regulation of the intracellular CoA concentration
	PANK1	Pantothenate kinase 1	226649_at	Down	Physiological regulation of the intracellular CoA concentration
	VNN1	Vanin 1	205844_at	Down	Membrane-associated proteins
	ACSL5	Acyl-CoA synthetase long-chain family member 5	222592_s_at	Down	Synthesis of cellular lipids and degradation via β-oxidation
	ACOT1	Acyl-CoA thioesterase 1	202982_s_at	Down	Catalyses the hydrolysis of acyl-CoAs to the NEFA and coenzyme A
	ACOT2	Acyl-CoA thioesterase 2	202982_s_at	Down	Catalyses the hydrolysis of acyl-CoAs to the NEFA and coenzyme A
	ENPP1	Ectonucleotide pyrophosphatase/ phosphodiesterase 1	229088_at	Down	Involved primarily in ATP hydrolysis at the plasma membrane
Phatidic acid pathway	*GPR63*	G protein-coupled receptor 63	220993_s_at	Up	Orphan receptor. May play a role in brain function
2-Oleoyl-glycerol_3-phosphate pathway	*LPAR1*	Lysophosphatidic acid receptor 1	204037_at	Up	Receptor for LPA, a mediator of diverse cellular activities

only cholesterol but also triacylglycerols in the liver, and upregulated the gene for sterol regulatory element binding protein (SREBP)-1c that governs fatty acid synthesis [3], probably via activation of liver-X-receptor (LXR) in the liver [25]. Therefore, in experimental models of high-cholesterol-diet-induced steatohepatitis, ezetimibe ameliorated liver steatosis by reducing cholesterol-induced activation of LXR and SREBP-1c [26, 27]. In the present study, however, treatment with ezetimibe unexpectedly ameliorated liver fibrosis staging and ballooning scores without significantly changing hepatic steatosis and insulin resistance.

One possible explanation for the improvement of hepatic fibrosis by ezetimibe treatment may be related to the direct effect of cholesterol on hepatic fibrogenesis. The cholesterol molecule affects membrane organisation and structure, which are critical determinants of membrane bilayer permeability and fluidity [28]. Altered cholesterol metabolism has several toxic effects on hepatocytes, resident macrophages, Kupffer cells and hepatic stellate cells, which promote NASH through diverse mechanisms. Hepatic stellate cells, in particular, are responsible for liver fibrosis in NASH. It has recently been reported that intracellular cholesterol accumulation directly activates hepatic stellated cells through a toll-like receptor-4-dependent pathway and triggers hepatic fibrosis [29]. These effects might be more evident in humans because, unlike rodents, where NPC1L1 is primarily expressed in the intestine, in humans *NPC1L1* mRNA is highly expressed both in the small intestine and liver. Therefore, ezetimibe is estimated to inhibit not only dietary and biliary cholesterol absorption through the small intestine, but also reabsorption of biliary cholesterol in the liver [30, 31]. Thus, ezetimibe may inhibit liver fibrosis by ameliorating

Table 5 Changes in plasma fatty acid composition

Fatty acid	Control		p^a	Ezetimibe		p^a	p^b
	Before	After		Before	After		
C12:0 (lauric acid)	1.9±0.5	1.2±0.2	0.177	2.3±0.6	2.1±0.5	0.753	0.301
C14:0 (myristic acid)	24.9±2.5	23.6±2.9	0.575	27.1±2.8	29.5±3.7	0.441	0.352
C16:0 (palmitic acid)	698.0±24.7	690.0±38.2	0.827	714.3±32.5	717.0±36.2	0.991	0.893
C16:1n-7 (palmitoleic acid)	68.6±6.5	72.5±9.6	0.643	62.4±5.0	69.9±6.2	0.219	0.721
C17:0 (margaric acid)	NE	NE		NE	NE		
C18:0 (stearic acid)	203.3±9.4	196.7±6.9	0.488	207.2±7.7	211.0±9.9	0.854	0.571
C18:1n-9 (oleic acid)	560.2±31.3	556.4±30.3	0.914	547.3±23.9	578.8±32.1	0.475	0.550
C18:2n-6 (linoleic acid)	745.8±26.3	750.6±34.4	0.910	735.8±34.2	713.5±31.4	0.558	0.629
C18:3n-6 (γ-linolenic acid)	9.8±1.3	9.2±1.0	0.506	9.8±0.9	11.1±1.5	0.402	0.300
C18:3n-3 (α-linolenic acid)	21.7±1.6	20.1±1.4	0.285	23.0±2.2	21.6±1.5	0.507	0.924
C20:0n-6 (arachidic acid)	7.0±0.4	6.9±0.3	0.671	7.2±0.2	7.0±0.3	0.410	0.642
C20:1n-9 (eicosenoic acid)	4.8±0.3	4.8±0.4	0.323	4.3±0.2	4.2±0.3	0.831	0.343
C20:2n-6 (eicosadienoic acid)	6.1±0.4	6.1±0.3	0.899	5.6±0.2	5.7±0.3	0.774	0.770
C20:3n-6 (dihomo-γ-linolenic acid)	36.6±3.0	37.3±2.8	0.784	36.5±2.4	40.6±3.7	0.247	0.438
C20:3n-9 (eicosatrienoic acid)	2.5±0.4	2.4±0.4	0.941	1.9±0.2	2.7±0.5	0.034	0.079
C20:4n-6 (arachidonic acid)	135.7±8.4	138.8±6.0	0.689	143.8±11.1	151.1±11.0	0.538	0.787
C20:5n-3 (eicosapentaenoic acid)	67.0±9.0	71.3±9.3	0.640	64.4±7.2	59.1±5.7	0.385	0.369
C22:0 (behenic acid)	16.6±0.8	18.3±1.0	0.035	17.1±0.8	17.9±1.3	0.623	0.468
C22:1n-9 (erucic acid)	1.6±0.1	1.3±0.1	0.066	1.3±0.1	1.3±0.1	0.914	0.170
C22:2n-6 (docosadienoic acid)	NE	NE		NE	NE		
C22:4n-6 (docosatetraenoic acid)	3.9±0.2	4.2±0.2	0.252	4.4±0.3	4.9±0.6	0.262	0.689
C22:5n-3 (docosapentaenoic acid)	20.0±1.4	20.7±1.7	0.657	20.7±1.7	21.5±1.7	0.839	0.887
C22:6n-3 (docosahexaenoic acid)	128.7±9.8	138.6±9.3	0.231	126.5±10.0	128.3±10.8	0.936	0.456
C24:1 (nervonic acid)	35.4±2.2	36.1±2.1	0.656	31.6±1.8	30.3±1.9	0.275	0.263

Data are expressed as means ± SE

[a] p value for the intergroup comparison (baseline vs 6 month)

[b] p value for the intergroup comparison (changes from baseline between groups)

NE, not estimated

cholesterol-induced activation of hepatic stellate cells in patients with NAFLD. This hypothesis was well supported by the hepatic gene expression profile induced by ezetimibe administration. Ezetimibe treatment coordinately downregulated genes involved in skeletal muscle development and cell adhesion molecules, suggesting that ezetimibe suppressed stellate cell development into myofibroblasts and thereby inhibited fibrogenesis.

Another important finding of the present study was that treatment with ezetimibe significantly deteriorated glycaemic control. Ezetimibe therapy also altered the hepatic profile of fatty acid components by significantly increasing hepatic levels of lauric, myristic, palmitic, palmitoleic, margaric, stearic, oleic and linoleic acids. Experimentally, palmitate induces interleukin-8 [32], endoplasmic reticulum stress, and c-Jun amino-terminal kinase activation and promotes apoptosis in the liver [5, 33, 34]. Lipid-induced oxidative stress and inflammation are closely related to insulin resistance [3, 5], which could be relevant to the ezetimibe-induced deterioration of glucose homeostasis. Indeed, urinary excretion of 8-isoprostanes was significantly increased in the ezetimibe group compared with the control, and showed significant negative correlation with insulin sensitivity indices such as the Matsuda index and QUICKI in the present study (ESM Table 6). Moreover, hepatic gene expression in the ezetimibe group showed coordinated upregulation of genes involved in the immune response compared with those in the control group, suggestive of oxidative stress caused by ezetimibe treatment.

Pathway analysis of the metabolic network showed unique metabolic changes in the ezetimibe group compared with the control group. In the control group, genes involved in the CoA-biosynthesis pathway were coordinately downregulated, and those in the glycerol-3 phosphate pathway coordinately upregulated, suggesting activated triacylglycerols biosynthesis. In the ezetimibe group,